Available online at www.sciencedirect.com
SCIENCE DIRECT®

Journal of Organometallic Chemistry 670 (2003) 17–26

Journal of Organometallic Chemistry

www.elsevier.com/locate/jorganchem

New ferrocenyl heterometallic complexes of 2,7-diethynylfluoren-9-one

Wai-Yeung Wong *, Ka-Yan Ho, Ka-Ho Choi

Department of Chemistry, Hong Kong Baptist University, Waterloo Road, Kowloon Tong, Hong Kong, PR China

Received 18 September 2002; received in revised form 18 October 2002; accepted 18 October 2002

Abstract

A new series of rigid-rod alkynylferrocenyl precursors with central fluoren-9-one bridge, 2-bromo-7-(2-ferrocenylethynyl)fluoren-9-one (**1b**), 2-trimethylsilylethynyl-7-(2-ferrocenylethynyl)fluoren-9-one (**2**) and 2-ethynyl-7-(2-ferrocenylethynyl)fluoren-9-one (**3**), have been prepared in moderate to good yields. The ferrocenylacetylene complex **3** can provide a direct access to novel heterometallic complexes, *trans*-$[(\eta^5\text{-}C_5H_5)Fe(\eta^5\text{-}C_5H_4)C{\equiv}CRC{\equiv}CPt(PEt_3)_2Ph]$ (**4**), *trans*-$[(\eta^5\text{-}C_5H_5)Fe(\eta^5\text{-}C_5H_4)C{\equiv}CRC{\equiv}CPt(PBu_3)_2C{\equiv}CRC{\equiv}C(\eta^5\text{-}C_5H_4)Fe(\eta^5\text{-}C_5H_5)]$ (**5**), $[(\eta^5\text{-}C_5H_5)Fe(\eta^5\text{-}C_5H_4)C{\equiv}CRC{\equiv}CAu(PPh_3)]$ (**6**) and $[(\eta^5\text{-}C_5H_5)Fe(\eta^5\text{-}C_5H_4)C{\equiv}CRC{\equiv}CHgMe]$ (**7**) (R=fluoren-9-one-2,7-diyl), following the CuI-catalyzed dehydrohalogenation reactions with the appropriate metal chloride compounds. All the new complexes have been characterized by FTIR, ^{1}H-NMR and UV–vis spectroscopies and fast atom bombardment mass spectrometry. The solid state molecular structures of **3**, **5**, **6** and **7** have been established by X-ray crystallography. The redox chemistry of these mixed-metal species has been investigated by cyclic voltammetry and oxidation of the ferrocenyl moiety is facilitated by the presence of the heavy metal centre and increased conjugation in the chain through the ethynyl and fluorenone linkage units.

Keywords: Alkynyl complexes; Ferrocene; Gold; Mercury; Platinum

1. Introduction

There is an upsurge of interest in the research community in the molecular design and synthesis of carbon-rich bi- or multi-metallic assemblies containing π-conjugated chains [1]. It has been demonstrated that molecular wires comprising mixed-valence bimetallic fragments or remote redox-active organometallic building blocks linked by all-carbon chains could be used in molecular electronics, optoelectronic devices and chemical sensing appliances [2]. Two common models are being used to evaluate the capability of electronic communication between two metal centres 'M_1' at the termini made feasible by an organic spacer 'M_1–spacer–M_1', and the effect of another organometallic fragment 'M_2' in a conjugated organic chain 'M_1–spacer–M_2–spacer–M_1' [3]. Several systems where redox active sites are strongly coupled electronically through the polyynyl fragments have been reported [3]. With this research framework in mind, much efforts have particularly been devoted to the synthesis of ferrocene-based homo- and heterometallic materials with spacers such as oligoene, oligoyne, thiophene, furan, phenylene, phenyleneyne, thienyl ethynyl and furanyl vinyl units [3,4].

Considerable current attention is paid to the organic and metal-based materials incorporated with fluorene auxiliaries [5,6]. The ease of modification and knowledge of the structure–property relationship of polyfluorene homopolymers and copolymers continue to make the fluorene-functionalized compounds very at-

---

* Corresponding author. Tel.: +852-3411-7074; fax: +852-3411-7348
E-mail address: rwywong@hkbu.edu.hk (W.-Y. Wong).

0022-328X/02/$ - see front matter © 2002 Elsevier Science B.V. All rights reserved.
PII: S0022-328X(02)02069-7

tractive candidates in the development of new functional materials [5a,5f]. Recently, a comprehensive program was therefore launched in our laboratory to prepare a range of organometallic alkynyl compounds containing fluorenyl linkers [6]. Remarkable results on the importance of using fluorenyl derivatives in bi- and polymetallic species have encouraged us to design new heterometallic systems featuring this linking unit [5,6]. Following our recent report of the synthesis and properties of 2,7-bis(ferrocenylethynyl)fluoren-9-one and related species [6e], we report in this contribution the parallel chemistry of a series of fluorenone-containing heteronuclear organometallic alkynyl complexes end-capped with ferrocenyl entity and another transition metal.

2. Results and discussion

2.1. Synthesis

The reactions pertaining to the synthesis of our compounds in this study are summarized in Scheme 1. 2-Bromo-7-(2-ferrocenylethynyl)fluoren-9-one (**1b**) was prepared in the first step by the Sonogashira coupling reaction of ethynylferrocene with an excess of 2,7-dibromofluoren-9-one [6e,7]. Inevitably, this preparation was accompanied by the isolation of the known complex 2,7-bis(ferrocenylethynyl)fluoren-9-one (**1a**) as a minor product [6e]. We were able to prevent the formation of the homocoupling product 1,4-diferrocenylbutadiyne under strictly anaerobic conditions. The mono-bromo species **1b** can undergo similar cross-coupling reaction with trimethylsilylacetylene to give 2-trimethylsilylethynyl-7-(2-ferrocenylethynyl)fluoren-9-one (**2**) in good yield, which upon deprotection with K_2CO_3 in MeOH affords 2-ethynyl-7-(2-ferrocenylethynyl)fluoren-9-one (**3**) in high yield. With the free alkyne unit, compound **3** should be a favourable starting unit to the synthesis of new hetero-bimetallic and trimetallic systems. Following the typical dehydrohalogenation reactions between **3** and *trans*-[Pt(PEt$_3$)$_2$(Ph)Cl] or *trans*-[Pt(PBu$_3$)$_2$Cl$_2$] under the CuI–^{i}Pr$_2$NH conditions [6a,6b,6c,6d,7], a convenient route to new platinum(II) alkynyl complexes *trans*-[(η^5-C_5H_5)Fe(η^5-C_5H_4)C≡CRC≡CPt(PEt$_3$)$_2$Ph] (**4**) and *trans*-[(η^5-C_5H_5)Fe(η^5-C_5H_4)C≡CRC≡CPt(PBu$_3$)$_2$C≡CRC≡C(η^5-C_5H_4)Fe(η^5-C_5H_5)] (**5**) (R=fluoren-9-one-2,7-diyl) can be developed. These reaction steps were readily monitored by solution IR spectroscopy and thin-layer chromatography (TLC). All the complexes were purified by preparative TLC on silica using a hexane–CH_2Cl_2 mixture as eluent and they were isolated as air-stable orange to red solids in high purity. Treatment of **3** with Au(PPh$_3$)Cl or MeHgCl in an excess of basic MeOH produced the alkynylgold(I) complex [(η^5-C_5H_5)Fe(η^5-C_5H_4)C≡CRC≡CAu(PPh$_3$)] (**6**) and the alkynylmercury(II) complex [(η^5-C_5H_5)Fe(η^5-C_5H_4)C≡CRC≡CHgMe] (**7**) (R=fluoren-9-

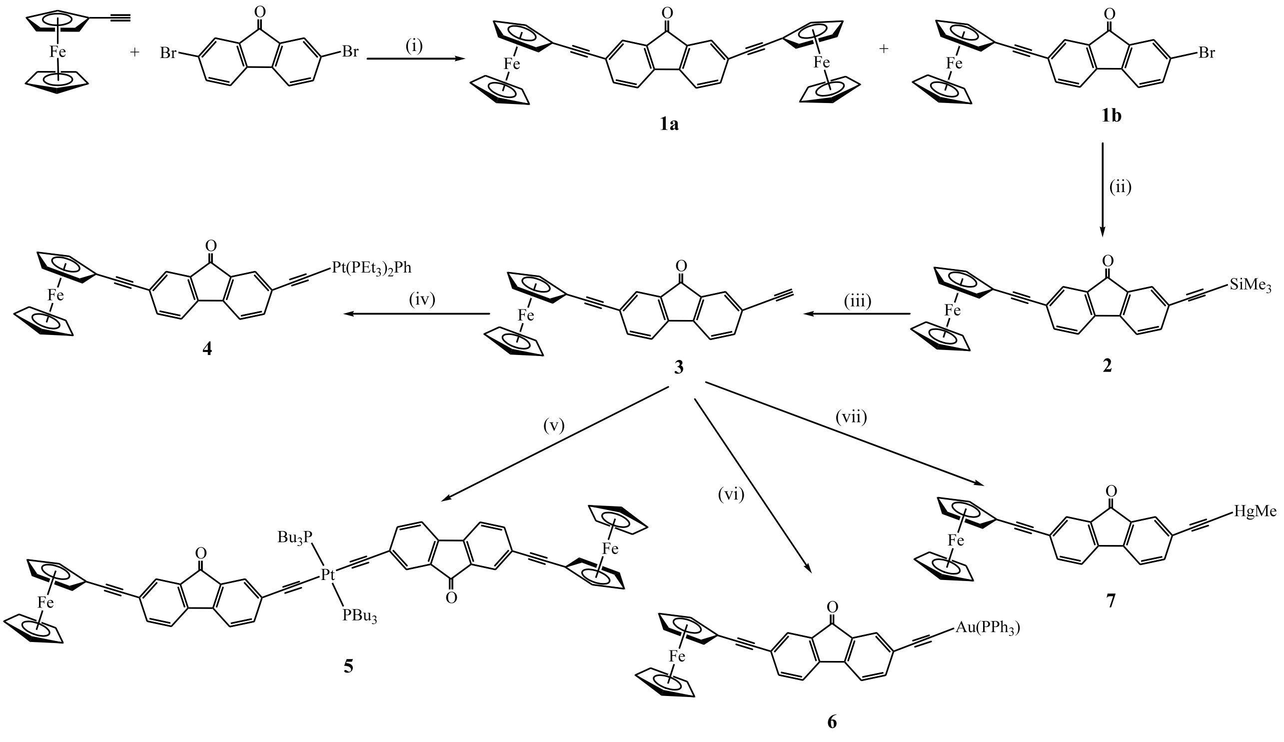

Scheme 1. (i) Pd(OAc)$_2$, CuI, PPh$_3$, ^{i}Pr$_2$NH; (ii) trimethylsilylacetylene, Pd(OAc)$_2$, CuI, PPh$_3$, ^{i}Pr$_2$NH; (iii) K_2CO_3, MeOH; (iv) *trans*-[Pt(PEt$_3$)$_2$(Ph)Cl], CuI, ^{i}Pr$_2$NH; (v) *trans*-[Pt(PBu$_3$)$_2$Cl$_2$] (0.5 equiv.), CuI, ^{i}Pr$_2$NH; (vi) Au(PPh$_3$)Cl, NaOMe, MeOH; (vii) MeHgCl, NaOMe, MeOH.

one-2,7-diyl), which readily precipitated from the solution mixture [6f,8]. All complexes are soluble in common organic solvents and have been characterized by satisfactory microanalysis, fast atom bombardment mass spectrometry (FABMS), IR and NMR spectroscopies.

2.2. Spectroscopic properties

All the new compounds display weak to moderate IR stretching vibrations for the C≡C moieties in the frequency range 2089–2213 cm^{-1}. In general, two ν(C≡C) bands are observed in the spectra of **2**–**7**. Those at the higher frequencies absorb at similar energies in each case and compare well with the value (ca. 2211 cm^{-1}) found in **1a** [6e]. The lower frequency ν(C≡C) band appears lower in energy for **4** and **5** than that found in the uncoordinated precursor **3**, suggesting the back-bonding effect of the Pt(II) centre to the acetylide. Apparently, the spectral pattern in the ν(C≡C) region for **6** and **7** is a combination of those for their homometallic binuclear congeners, **1a** and $[(Ph_3P)AuC{\equiv}CRC{\equiv}CAu(PPh_3)]$ (2107 cm^{-1}) or [MeHgC≡CRC≡CHgMe] (2127 cm^{-1}) (R=fluoren-9-one-2,7-diyl) [6e,6f]. The C≡*C*–*H* stretching band also occurs at 3294 cm^{-1} for **3**. In each case, characteristic ν(C=O) IR vibration due to the fluorenone unit was also observed at around 1720 cm^{-1}. In the ^{1}H-NMR spectra, proton signals due to the fluorenone and other organic groups were observed. The ferrocenyl unit also gives rise to a strong singlet for the C_5H_5 ring and an unsymmetrical pair of pseudo triplets for the C_5H_4 ring, typical of other monosubstituted ferrocene. For **5**, the symmetrical nature of the complex was confirmed by the NMR spectral pattern. The room temperature ^{31}P-NMR signals of the platinum-containing compounds **4** and **5** are detected as a sharp singlet flanked by platinum satellites, in agreement with a *trans* configuration of the bound phosphine ligands. The ^{31}P-NMR resonance for **6** is close to the value encountered for $[(Ph_3P)AuC{\equiv}CRC{\equiv}CAu(PPh_3)]$ (δ 43.55) [6f]. The formulae of these compounds were successfully established by the intense molecular ion peak in each of the FABMS.

The absorption spectral data of our new complexes were recorded in CH_2Cl_2 and the data are given in Table 1. Except for the trimetallic compound **5**, each of them essentially displays three main structureless absorption bands. As observed for other similar systems, the higher energy intense bands below 400 nm in the near UV region are likely to arise from π–π* electronic transition of the fluorenone group [6a,6e]. The broad low-energy features account for the orange to red colors of these ferrocenyl compounds. Introduction of the platinum(II) segment in **4** and **5** is found to red-shift the lowest energy bands and to increase the absorption intensity, suggesting an enhancement in the extent of π-delocalization through the platinum conjugated system that is fully consistent with the IR data. A bathochromic shift of about 20 nm is observed from **3** to **4** and **5**. These data may also imply an additional charge–transfer character due to the platinum centre, in line with the recently reported compounds incorporating oligothienyl-bridging units [7,9]. However, apart from an increase in the molar extinction coefficients, there is no significant variation in the lowest energy peak from **3** to **6** and **7**.

Table 1
UV–vis and electrochemical data for new complexes in CH_2Cl_2

Complex	λ_{max} (nm) [a]	$E_{1/2}$ (V) [b]
1a [c]	288 (8.7), 349 (4.7), 493 (0.8)	0.14 (159), −0.95 [d]
1b	279 (5.3), 338 (1.8), 472 (0.3)	0.17 (199), −0.74 [d]
2	288 (3.7), 341 (1.3), 467 (0.2)	0.13 (80), −0.77 [d]
3	284 (7.3), 344 (2.3), 474 (0.1)	0.17 (159), −0.73 [d]
4	272 sh (1.9), 298 (2.4), 307 (2.4), 368 (2.5), 496 (0.3)	0.71 [d], 0.12 (99)
5	297 (7.1), 372 (8.2), 494 (1.1)	0.88 [d], 0.11 (139)
6	297 (6.7), 349 (3.4), 476 (0.3)	0.13 (139)
7	289 (7.8), 343 (3.1), 474 (0.4)	0.14 (120)

[a] Extinction coefficients ($\varepsilon \times 10^{-4}$ dm^3 mol^{-1} cm^{-1}) are shown in parentheses.

[b] Scan rate = 100 mV s^{-1}, half-wave potential values $E_{1/2} = (E_{pa} + E_{pc})/2$ for reversible oxidation, $\Delta E_p = E_{pa} - E_{pc}$ (in mV) for reversible waves are given in parentheses, where E_{pa} and E_{pc} are the anodic and cathodic peak potentials, respectively.

[c] Data from Ref. [6e].

[d] Irreversible wave.

2.3. Electrochemistry

The electrochemical properties of complexes **1**–**7** were studied in CH_2Cl_2 at room temperature by means of cyclic voltammetry and the redox data are collected in Table 1. In each case, the complex is electroactive and the cyclic voltammogram is dominated by one quasi-reversible oxidation wave due to the ferrocenyl electrophore that is present. An anodic shift of the ferrocene–ferrocenium couple relative to the ferrocene standard is caused by the unsaturation of the ethynyl groups which renders the removal of electrons more difficult. When the conjugation length is increased from **3** to **4**–**7** upon capping the end group with an organometallic segment, oxidation is favoured by the delocalization of charge along the main chain through a $d_\pi \rightarrow p_\pi$ interaction which leads to a lowering of the oxidation potentials. The most significant cathodic shift of ca. 0.06 V (from 0.17 V in **3** to 0.11 V in **5**) is noted in the most extended Fe–Pt–Fe complex **5**, however, the two ferrocenyl end groups do not exhibit an observable electronic communication through the fluorenyl ring system in such case. Considering the relative peak heights with respect to the added ferrocene standard in the cyclic voltammogram, complex **5** only undergoes a single-step two-electron oxidation involving the concomitant oxidation of the two ferrocenyl subunits at a scan rate of 100 mV s^{-1}. Non-interacting diferrocenyl systems have previously been reported for *trans*-$[(\eta^5\text{-}C_5H_5)Fe(\eta^5\text{-}C_5H_4)C\equiv CPt(PR_3)_2C\equiv C(\eta^5\text{-}C_5H_4)Fe(\eta^5\text{-}C_5H_5)]$ [10], *trans*-$[Pd(PBu_3)_2\{C\equiv CC_6H_4C\equiv C(\eta^5\text{-}C_5H_4)Fe(\eta^5\text{-}C_5H_5)\}_2]$ [3a] and *trans*-$[(\eta^5\text{-}C_5H_5)Fe(\eta^5\text{-}C_5H_4)C\equiv C(C_4H_2S)_mC\equiv CPt(PBu_3)_2C\equiv C(C_4H_2S)_mC\equiv C(\eta^5\text{-}C_5H_4)Fe(\eta^5\text{-}C_5H_5)]$ ($m = 1$–3) [7]. The $E_{1/2}$ value is slightly more anodic in **7** than in **6** because of the higher formal oxidation state of mercury(II) than that of gold(I), which would hinder the back-donation to π* in the former case.

Another redox event was also detected at higher positive potentials in **4** and **5**, which was absent in the remaining complexes. We assign this to the irreversible oxidation of the platinum moiety [Pt(II) → Pt(III)]. Fluorenone-based reduction waves were only encountered for the precursors **1b**, **2** and **3** without the heavy metal groups, which appear in the narrow range of 0.73–0.77 V.

2.4. Crystal structure analyses

The molecular structures of complexes **3**, **5**, **6** and **7**, as determined by X-ray analyses, are depicted in Figs. 1–4, respectively. Pertinent bond parameters along with some dihedral angles are listed in Tables 2–5. There are two independent molecules per asymmetric unit in the unit cell of **3** and each molecule consists of one ferrocene unit appended to one end of 2,7-diethynylfluoren-9-one, leaving a terminal alkyne moiety at the other end. The C(11)–C(12) distance is typical at 1.186(4)–1.192(4) Å whereas the free alkyne C(26)–C(27) bond length appears slightly shorter at 1.160(5)–1.174(4) Å due to the libration effect [11]. For **5**, there is a centrosymmetry at the platinum centre and the crystal structure shows a diferrocenyl end-capped species in which two deprotonated forms of **3** are bonded to a $Pt(PBu_3)_2$ unit in a *trans* geometry to afford a rigid-rod molecule with an iron–iron through-space separation of about 34 Å. The corresponding mean Fe–Pt distance is ca. 17 Å. The platinum centre is square-planar with four ligand groups in the coordination sphere and the Pt–P distance is 2.2981(10) Å. The alkynyl bond lengths span the narrow range of 1.169(3)–1.189(3) Å, which are comparable to those found in the bithienyl-linked analogue [7]. The nearly linear bond angles around the alkyne units conform to the rigid and straight-chain nature of the molecule. There are no short intermolecular contacts or π-stacking of fluorenone units in the lattice of **5**.

The structures of **6** and **7** belong to new heterometallic compounds in which the isoelectronic fragments $Au(PPh_3)$ and MeHg are each attached to the terminal alkyne entity of 2-ethynyl-7-(2-ferrocenylethynyl)fluoren-9-one, respectively. Variation of the end groups in both cases does not have a great influence on the bond parameters of the fluorenone unit. The geometry about the Au(I) and Hg(II) centres is essentially linear and the mean P–Au–C angle of 178.1(3)° and Au–C–C angle of 177.7(8)° in **6** as well as the C–Hg–C angle of 179.0(4)° and Hg–C–C angle of 178.5(9)° are indicative of sp hybridization in the metal atom and acetylenic carbon [6f]. For **6**, two independent molecules are associated with the asymmetric unit in the unit cell and the average Au–P bond length of 2.270 Å is similar to those observed in other alkynylgold(I) phosphines [6f,8d,8e,8f,8g]. The alkynyl bond distances are characteristic of other structurally similar metal acetylides [6f,8d,8e,8f,8g]. However, no short Au···Au intermolecular interactions are observed in the solid state of **6**, presumably because the sterically bulky ferrocenyl and phenyl groups prevent the close approach of molecules. We note that the nearest intermolecular contact arises from the hydrogen bonding interaction between oxygen of the fluorenone ring and hydrogen on C-8 of the adjacent molecule (O(1B)···H(70A) 2.549 Å; O(2A)···H(25B) 2.466 Å). Intermolecular Au···H interactions are also observed between gold atom and hydrogen

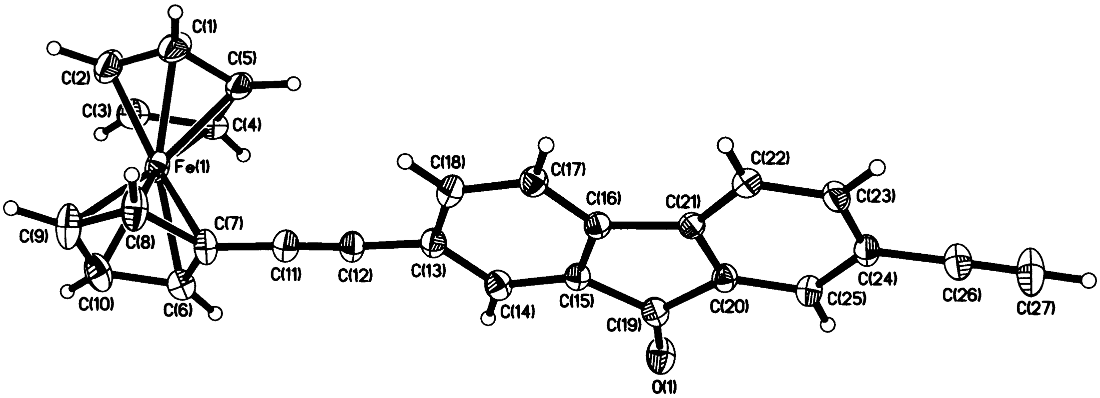

Fig. 1. A perspective view of one molecule of **3**, showing the atomic labelling scheme. Thermal ellipsoids were drawn at the 25% probability level.

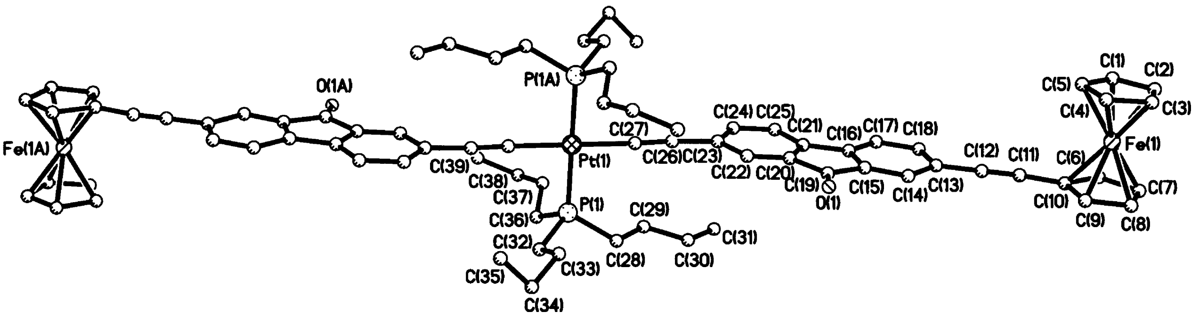

Fig. 2. A perspective view of **5**, showing the atomic labelling scheme. Hydrogen atoms were omitted for clarity.

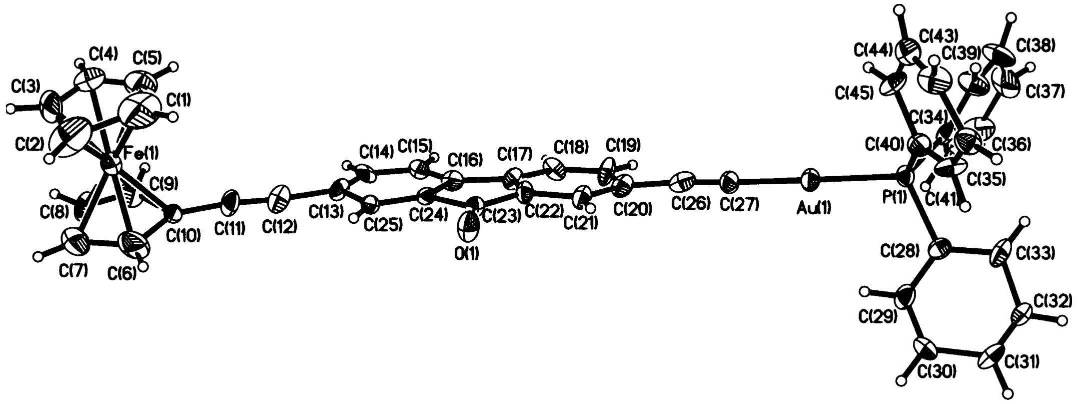

Fig. 3. A perspective view of one molecule of **6**, showing the atomic labelling scheme. Thermal ellipsoids were drawn at the 25% probability level.

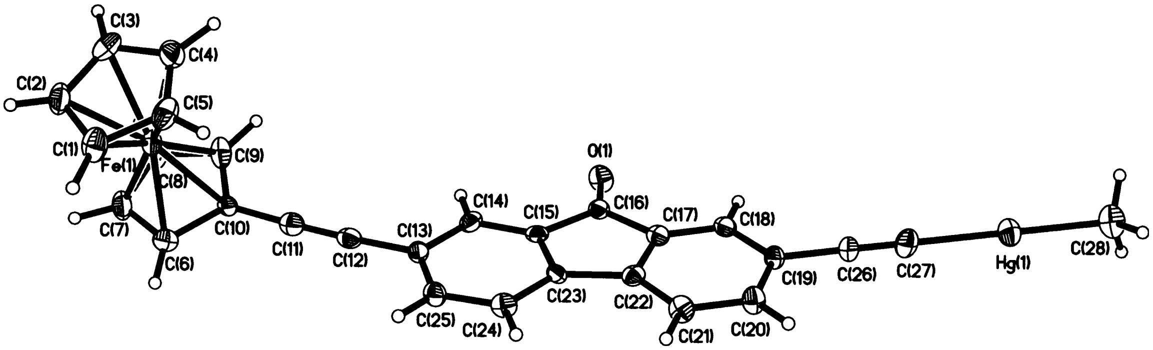

Fig. 4. A perspective view of **7**, showing the atomic labelling scheme. Thermal ellipsoids were drawn at the 25% probability level.

Table 2
Selected bond lengths (Å) and angles (°) for complex **3**

	Molecule 1	Molecule 2		Molecule 1	Molecule 2
Fe(1)–C(1)	2.054(3)	2.034(3)	Fe(1)–C(2)	2.040(3)	2.024(3)
Fe(1)–C(3)	2.042(3)	2.021(3)	Fe(1)–C(4)	2.038(3)	2.030(3)
Fe(1)–C(5)	2.039(3)	2.044(3)	Fe(1)–C(6)	2.049(3)	2.031(3)
Fe(1)–C(7)	2.060(3)	2.042(3)	Fe(1)–C(8)	2.032(3)	2.037(3)
Fe(1)–C(9)	2.037(3)	2.035(3)	Fe(1)–C(10)	2.045(3)	2.020(3)
C(11)–C(12)	1.186(4)	1.192(4)	C(26)–C(27)	1.160(5)	1.174(4)
C(11)–C(12)–C(13)	177.0(3)	178.9(3)	C(24)–C(26)–C(27)	179.1(4)	177.0(4)
Dihedral angles (°) between planes					
A and B	1.6	2.0	A and C	5.5	7.7
B and C	5.2	7.8			

Planes: A, C(1)–C(2)–C(3)–C(4)–C(5); B, C(6)–C(7)–C(8)–C(9)–C(10); C, C(13)–C(14)–C(15)–C(16)–C(17)–C(18)–C(19)–C(20)–C(21)–C(22)–C(23)–C(24)–C(25).

Table 3
Selected bond lengths (Å) and angles (°) for complex **5**

Fe(1)–C(1)	2.006(4)	Fe(1)–C(2)	2.021(3)		
Fe(1)–C(3)	2.032(3)	Fe(1)–C(4)	2.039(3)		
Fe(1)–C(5)	2.026(3)	Fe(1)–C(6)	2.038(2)		
Fe(1)–C(7)	2.042(2)	Fe(1)–C(8)	2.043(2)		
Fe(1)–C(9)	2.023(2)	Fe(1)–C(10)	2.0413(18)		
C(11)–C(12)	1.189(3)	C(26)–C(27)	1.169(3)		
Pt(1)–C(27)	2.012(2)	Pt(1)–P(1)	2.2981(10)		
C(11)–C(12)–C(13)	176.8(2)	C(23)–C(26)–C(27)	174.7(2)		
Pt(1)–C(27)–C(26)	178.33(18)	P(1)–Pt(1)–C(27)	93.63(6)		
Dihedral angles (°) between planes					
A and B	0.5	A and C	1.5	B and C	1.2

Planes: A, C(1)–C(2)–C(3)–C(4)–C(5); B, C(6)–C(7)–C(8)–C(9)–C(10); C, C(13)–C(14)–C(15)–C(16)–C(17)–C(18)–C(19)–C(20)–C(21)–C(22)–C(23)–C(24)–C(25).

Table 4
Selected bond lengths (Å) and angles (°) for complex **6**

	Molecule 1	Molecule 2		Molecule 1	Molecule 2
Fe(1)–C(1)	2.061(12)	1.941(14)	Fe(1)–C(2)	1.962(18)	1.991(14)
Fe(1)–C(3)	2.014(9)	2.057(11)	Fe(1)–C(4)	2.041(10)	1.999(14)
Fe(1)–C(5)	2.019(10)	1.951(11)	Fe(1)–C(6)	2.002(11)	2.104(13)
Fe(1)–C(7)	2.108(13)	1.965(17)	Fe(1)–C(8)	2.058(7)	2.029(9)
Fe(1)–C(9)	1.946(10)	2.018(7)	Fe(1)–C(10)	2.030(7)	1.995(10)
C(11)–C(12)	1.178(11)	1.192(10)	C(26)–C(27)	1.161(11)	1.240(11)
Au(1)–C(27)	1.970(7)	1.989(8)	Au(1)–P(1)	2.2724(17)	2.268(2)
C(11)–C(12)–C(13)	175.9(9)	174.7(7)	C(20)–C(26)–C(27)	174.6(8)	175.2(9)
P(1)–Au(1)–C(27)	178.7(3)	177.5(3)	Au(1)–C(27)–C(26)	177.1(8)	178.3(8)
Dihedral angles (°) between planes					
A and B	2.5	3.9	A and C	19.9	15.9
B and C	18.1	17.8			

Planes: A, C(1)–C(2)–C(3)–C(4)–C(5); B, C(6)–C(7)–C(8)–C(9)–C(10); C, C(13)–C(14)–C(15)–C(16)–C(17)–C(18)–C(19)–C(20)–C(21)–C(22)–C(23)–C(24)–C(25).

Table 5
Selected bond lengths (Å) and angles (°) for complex **7**

Fe(1)–C(1)	2.031(10)	Fe(1)–C(2)	2.054(9)		
Fe(1)–C(3)	2.072(10)	Fe(1)–C(4)	2.082(10)		
Fe(1)–C(5)	2.057(10)	Fe(1)–C(6)	2.014(9)		
Fe(1)–C(7)	2.026(10)	Fe(1)–C(8)	2.043(10)		
Fe(1)–C(9)	2.009(9)	Fe(1)–C(10)	2.025(8)		
C(11)–C(12)	1.222(12)	C(26)–C(27)	1.157(11)		
Hg(1)–C(27)	2.050(10)	Hg(1)–C(28)	2.041(9)		
C(11)–C(12)–C(13)	177.2(10)	C(19)–C(26)–C(27)	178.9(11)		
C(27)–Hg(1)–C(28)	179.0(4)	Hg(1)–C(27)–C(26)	178.5(9)		
Dihedral angles (°) between planes					
A and B	3.5	A and C	25.6	B and C	22.4

Planes: A, C(1)–C(2)–C(3)–C(4)–C(5); B, C(6)–C(7)–C(8)–C(9)–C(10); C, C(13)–C(14)–C(15)–C(16)–C(17)–C(18)–C(19)–C(20)–C(21)–C(22)–C(23)–C(24)–C(25).

atoms on the phenyl and ferrocenyl units (Au(1A)···H(89A) 3.053; Au(2A)···H(44A) 3.187; Au(2A)···H(2AB) 3.110 Å). Likewise, there are no apparent weak intermolecular Hg···Hg interactions or π-stacking of the aromatic rings in **7**. The closest intermolecular contacts in **7** are attributed to the Hg(1)···O(1) (3.314 Å) and Hg(1)···H(6A) (3.224 Å) interactions. The Hg–C(alkyne) bond (Hg(1)–C(27) 2.050(10) Å) appears longer than the Au–C(alkyne) bond in **6** but matches with those in other known Hg(II) acetylide complexes

[12]. The Hg–CH_3 bond (2.041(9) Å) is comparable to those of other related systems [13]. In all cases, the fluorenonediyl ring system is planar and the cyclopentadienyl rings of the ferrocenyl group are almost parallel with tilt angles lying in the range 0.5–3.9°.

3. Concluding remarks

A new class of heterometallic bis- and poly(alkynyl) complexes end-capped with a ferrocenyl moiety and another transition metal (e.g. platinum, gold and mercury) have been prepared in good yields. These compounds were fully characterized by spectroscopic, electrochemical and structural methods. Our results show that delocalization of π electrons continues through the metal centre to different extent and the conjugation is greater for the Pt(II) complexes than the Au(I) and Hg(II) species. The production of the trimetallic acetylide complex **5** with a metal–metal through-space distance of over 3 nm provides us an opportunity to investigate novel materials of nano-sized dimensions and we are currently extending these promising synthetic paths in the search for a new series of diacetylenic-based materials and other oligomeric homologues of longer chain length and more repeat units.

4. Experimental

4.1. General procedures

All reactions were carried out under N_2 with the use of standard inert atmosphere and Schlenk techniques, but no special precautions were taken to exclude oxygen during work-up. Solvents were predried and distilled from appropriate drying agents [14]. All chemicals, unless otherwise stated, were obtained from commercial sources and used as received. Preparative TLC was performed on 0.7 mm silica plates (Merck Kieselgel 60 GF_{254}) prepared in our laboratory. The starting compounds ethynylferrocene [15], *trans*-$[Pt(PEt_3)_2(Ph)Cl]$ [16] and *trans*-$[Pt(PBu_3)_2Cl_2]$ [17] were prepared by the reported procedures. Infrared spectra were recorded as CH_2Cl_2 solutions in a CaF_2 cell (0.5 mm path length) on a Perkin–Elmer Paragon 1000 PC or Nicolet Magna 550 Series II FTIR spectrometer. Proton NMR spectra were measured in $CDCl_3$ on a JEOL EX270 or a Varian INOVA 400 MHz FT NMR spectrometer. Chemical shifts were quoted relative to $SiMe_4$ (δ 0). Fast atom bombardment mass spectra were recorded on a Finnigan MAT SSQ710 mass spectrometer. Electronic absorption spectra were obtained with a Hewlett Packard 8453 UV–vis spectrometer. Cyclic voltammetry experiments were done with a Princeton Applied Research model 273A potentiostat. A conventional three-electrode configuration consisting of a glassy-carbon working electrode, a Pt-wire counter electrode and a Ag–$AgNO_3$ reference electrode (0.1 M in acetonitrile) was used. The solvent in all measurements was deoxygenated CH_2Cl_2 and the supporting electrolyte was 0.1 M $[Bu_4N]PF_6$. Ferrocene was added as a calibrant after each set of measurements and all potentials reported were quoted with reference to the ferrocene–ferrocenium couple (taken as $E_{1/2} = +0.17$ V relative to Ag–$AgNO_3$). The number of electrons transferred for each compound was estimated by comparing the peak height of the respective ferrocene oxidation wave with an equal concentration of the ferrocene standard added in the same system, in which one-electron oxidation was assumed.

4.2. Preparations of complexes

*4.2.1. Synthesis of $[(\eta^5\text{-}C_5H_5)Fe(\eta^5\text{-}C_5H_4)C{\equiv}CRBr]$ (R=fluoren-9-one-2,7-diyl) (**1b**)*

2,7-Dibromofluoren-9-one (50 mg, 0.15 mmol) and ethynylferrocene (32 mg, 0.15 mmol) in $^iPr_2NH$–CH_2Cl_2 (30 cm^3, 1:1, v/v) were mixed under N_2 with catalytic amounts of $Pd(OAc)_2$ (1 mg), CuI (1 mg) and PPh_3 (2 mg). The mixture was allowed to reflux for a period of 15 h, after which all volatile components were removed under reduced pressure. The residue was redissolved in CH_2Cl_2 and subsequently subjected to preparative TLC separation on silica using hexane–CH_2Cl_2 (2:1, v/v) as eluent. The orange product **1b** ($R_f = 0.37$) was obtained in 45% yield (32 mg), accompanied by 20% of the known compound 2,7-bis(ferrocenylethynyl)fluoren-9-one (**1a**) ($R_f = 0.27$). IR (CH_2Cl_2): 2213 ν(C≡C), 1721 ν(C=O) cm^{-1}. ^1H-NMR ($CDCl_3$): δ 4.25 (s, 5H, C_5H_5), 4.27 (t, 2H, $J_{H\text{–}H} = 1.8$ Hz, C_5H_4), 4.52 (t, 2H, $J_{H\text{–}H} = 1.8$ Hz, C_5H_4), 7.38 (d, 1H, $J_{H\text{–}H} = 7.8$ Hz, fluorenone), 7.45 (d, 1H, $J_{H\text{–}H} = 7.8$ Hz, fluorenone), 7.57–7.63 (m, 2H, fluorenone) and 7.74–7.76 (m, 2H, fluorenone). FABMS: *m/z* 468 (M^+). Anal. Found: C, 64.02; H, 3.10. Calc. for $C_{25}H_{15}BrFeO$: C, 64.28; H, 3.24%.

*4.2.2. Synthesis of $[(\eta^5\text{-}C_5H_5)Fe(\eta^5\text{-}C_5H_4)C{\equiv}CRC{\equiv}CSiMe_3]$ (R=fluoren-9-one-2,7-diyl) (**2**)*

A mixture of **1b** (46 mg, 0.10 mmol), $Me_3SiC{\equiv}CH$ (20 g, 0.20 mmol) and freshly distilled $^iPr_2NH$ (15 cm^3) combined with catalytic quantities of $Pd(OAc)_2$ (1.5 mg), CuI (1.5 mg) and PPh_3 (3 mg) in CH_2Cl_2 (15 cm^3) were allowed to reflux for 17 h. The red residue obtained by removing the volatile components in vacuo was redissolved in CH_2Cl_2. Upon filtration through a short silica pad, the filtrate was concentrated and purified by preparative TLC ($R_f = 0.30$) using hexane–CH_2Cl_2 (2:1, v/v) as eluent to yield **2** as an orange solid (46 mg, 95%). IR (CH_2Cl_2): 2213, 2153 ν(C≡C), 1721 ν(C=O) cm^{-1}.

^{1}H-NMR ($CDCl_3$): δ 0.27 (s, 9H, Me), 4.26 (s, 5H, C_5H_5), 4.28 (t, 2H, $J_{H-H} = 1.2$ Hz, C_5H_4), 4.52 (t, 2H, $J_{H-H} = 1.2$ Hz, C_5H_4), 7.46 (d, 1H, $J_{H-H} = 7.6$ Hz, fluorenone), 7.47 (d, 1H, $J_{H-H} = 7.6$ Hz, fluorenone), 7.58–7.62 (m, 2H, fluorenone) and 7.74–7.78 (m, 2H, fluorenone). FABMS: *m/z* 484 (M^+). Anal. Found: C, 74.10; H, 4.69. Calc. for $C_{30}H_{24}FeOSi$: C, 74.38; H, 4.99%.

4.2.3. *Synthesis of [(η^5-C_5H_5)Fe(η^5-C_5H_4)C≡CRC≡CH] (R=fluoren-9-one-2,7-diyl) (**3**)*

To a solution of **2** (24 mg, 0.05 mmol) in Et_2O (10 cm^3) was added K_2CO_3 (7 mg, 0.05 mmol) in MeOH (15 cm^3). The mixture was stirred at room temperature (r.t.) for 24 h. After evaporation of the solvent, the crude product was dissolved in CH_2Cl_2 and chromatographed on silica plates ($R_f = 0.25$) eluting with hexane–CH_2Cl_2 (2:1, v/v) to afford pure **3** as a red powder in 92% yield (19 mg). IR (CH_2Cl_2): 3294 ν(≡CH), 2209, 2106 ν(C≡C), 1721 ν(C=O) cm^{-1}. ^{1}H-NMR ($CDCl_3$): δ 3.19 (s, 1H, C≡CH), 4.30 (m, 7H, $C_5H_5+C_5H_4$), 4.56 (t, 2H, $J_{H-H} = 1.8$ Hz, C_5H_4), 7.48 (d, 2H, $J_{H-H} = 7.2$ Hz, fluorenone), 7.58–7.63 (m, 2H, fluorenone) and 7.76 (m, 2H, fluorenone). FABMS: *m/z* 412 (M^+). Anal. Found: C, 78.35; H, 3.68. Calc. for $C_{27}H_{16}FeO$: C, 78.66; H, 3.91%.

4.2.4. *Synthesis of trans-[(η^5-C_5H_5)Fe(η^5-C_5H_4)C≡CRC≡CPt(PEt_3)$_2$Ph] (R=fluoren-9-one-2,7-diyl) (**4**)*

Compound **3** (82 mg, 0.20 mmol) and *trans*-[Pt(PEt_3)$_2$(Ph)Cl] (113 mg, 0.20 mmol) were dissolved in ^{i}Pr$_2$NH (15 cm^3) and CH_2Cl_2 (15 cm^3). After the addition of CuI (1.5 mg), the red solution was stirred at r.t. over 18 h. Concentration of the solution and subsequent purification by silica TLC ($R_f = 0.38$) using hexane–CH_2Cl_2 (2:1, v/v) as eluent readily led to the isolation of the title product **4** as a red–orange crystalline solid in 56% yield (103 mg). IR (CH_2Cl_2): 2209, 2089 ν(C≡C), 1717 ν(C=O) cm^{-1}. ^{1}H-NMR ($CDCl_3$): δ 1.08–1.12 (m, 18H, CH_3), 1.73–1.77 (m, 12H, CH_2), 4.25 (m, 7H, $C_5H_5+C_5H_4$), 4.51 (t, 2H, $J_{H-H} = 1.8$ Hz, C_5H_4), 6.81 (t, 1H, $J_{H-H} = 7.2$ Hz, H_{para} of Ph), 6.97 (t, 2H, $J_{H-H} = 7.2$ Hz, H_{meta} of Ph), 7.33 (t, 2H, $J_{H-H} = 7.2$ Hz, H_{ortho} of Ph), 7.40 (m, 3H, fluorenone), 7.53–7.55 (m, 2H, fluorenone) and 7.72 (m, 1H, fluorenone). ^{31}P{^{1}H}-NMR ($CDCl_3$): δ 11.04 ($^1J_{Pt-P} = 2636$ Hz). FABMS: *m/z* 920 (M^+). Anal. Found: C, 58.44; H, 5.58. Calc. for $C_{45}H_{50}FeOP_2Pt$: C, 58.76; H, 5.48%.

4.2.5. *Synthesis of trans-[(η^5-C_5H_5)Fe(η^5-C_5H_4)C≡CRC≡CPt(PBu_3)$_2$C≡CRC≡C(η^5-C_5H_4)Fe(η^5-C_5H_5)] (R=fluoren-9-one-2,7-diyl) (**5**)*

The compound *trans*-[Pt(PBu_3)$_2$$Cl_2$] (20 mg, 0.03 mmol) and two molar equivalents of **3** (25 mg, 0.06 mmol) were stirred in a mixture of ^{i}Pr$_2$NH–CH_2Cl_2 (30 cm^3, 1:1, v/v) at r.t. in the presence of CuI (1.5 mg). Stirring was continued for 18 h and evaporation of the volatile components left behind a reddish residue, purification of which was accomplished by preparative TLC using hexane–CH_2Cl_2 (2:1, v/v) as eluent. From the red band ($R_f = 0.24$) was obtained product **5** and a pure sample was isolated in 56% yield (24 mg) after recrystallization from a hexane–CH_2Cl_2 mixture. IR (CH_2Cl_2): 2213, 2092 ν(C≡C), 1716 ν(C=O) cm^{-1}. ^{1}H-NMR ($CDCl_3$): δ 0.88–0.96 (m, 18H, CH_3), 1.44–1.49 (m, 12H, CH_2CH_3), 1.58–1.61 (m, 12H, PCH_2CH_2), 2.12–2.14 (m, 12H, PCH_2), 4.26 (m, 14H, $C_5H_5+C_5H_4$), 4.52 (t, 4H, $J_{H-H} = 1.2$ Hz, C_5H_4), 7.36–7.41 (m, 6H, fluorenone), 7.53–7.56 (m, 4H, fluorenone) and 7.72 (m, 2H, fluorenone). ^{31}P{^{1}H}-NMR ($CDCl_3$): δ 4.37 ($^1J_{Pt-P} = 2316$ Hz). FABMS: *m/z* 1422 (M^+). Anal. Found: C, 65.52; H, 5.68. Calc. for $C_{78}H_{84}Fe_2O_2P_2Pt$: C, 65.87; H, 5.95%.

4.2.6. *Synthesis of [(η^5-C_5H_5)Fe(η^5-C_5H_4)C≡CRC≡CAu(PPh_3)] (R=fluoren-9-one-2,7-diyl) (**6**)*

Au(PPh_3)Cl (30 mg, 0.06 mmol) in MeOH (15 cm^3) was mixed with compound **3** (25 mg, 0.06 mmol) in CH_2Cl_2 (5 cm^3). To this solution mixture was added 3 cm^3 of basic MeOH (0.60 mmol, prepared by dissolving 0.20 g of NaOH in 25 cm^3 of MeOH). Within a few minutes, a red solid precipitated from the homogeneous solution. After stirring for 2 h, the solid was collected by filtration, washed with MeOH and air-dried to furnish an analytically pure sample of **6** in very high yield (47 mg, 90%). IR (CH_2Cl_2): 2213, 2111 ν(C≡C), 1719 ν(C=O) cm^{-1}. ^{1}H-NMR ($CDCl_3$): δ 4.26 (s, 5H, C_5H_5), 4.27 (t, 2H, $J_{H-H} = 1.8$ Hz, C_5H_4), 4.52 (t, 2H, $J_{H-H} = 1.8$ Hz, C_5H_4) and 7.41–7.78 (m, 21H, fluorenone+Ph). ^{31}P{^{1}H}-NMR ($CDCl_3$): δ 43.19. FABMS: *m/z* 870 (M^+). Anal. Found: C, 61.88; H, 3.28. Calc. for $C_{45}H_{30}AuFeOP$: C, 62.09; H, 3.47%.

4.2.7. *Synthesis of [(η^5-C_5H_5)Fe(η^5-C_5H_4)C≡CRC≡CHgMe] (R=fluoren-9-one-2,7-diyl) (**7**)*

Addition of an excess of basic MeOH (0.50 mmol) to a mixture of MeHgCl (13 mg, 0.05 mmol) in MeOH (15 cm^3) and **3** (21 mg, 0.05 mmol) in CH_2Cl_2 (5 cm^3) at r.t. led to the precipitation of the desired product **7** as a fine red powder. The solvents were decanted after 2 h and the red solid was air-dried to give 52% yield (16 mg) of **7**. IR (CH_2Cl_2): 2210, 2134 ν(C≡C), 1717 ν(C=O) cm^{-1}. ^{1}H-NMR ($CDCl_3$): δ 0.73 (s, 3H, $^2J_{Hg-H} = 148.0$ Hz, Me), 4.25 (s, 5H, C_5H_5), 4.27 (t, 2H, $J_{H-H} = 1.9$ Hz, C_5H_4), 4.52 (t, 2H, $J_{H-H} = 1.9$ Hz, C_5H_4), 7.43–7.50 (m, 2H, fluorenone), 7.56–7.61 (m, 2H, fluorenone) and 7.72–7.77 (m, 2H, fluorenone). Anal. Found: C, 53.49; H, 2.80. Calc. for $C_{28}H_{18}FeHgO$: C, 53.65; H, 2.89%.

Table 6
Summary of crystal structure data for complexes **3**, **5**, **6**and **7**

	3	5	6	7
Empirical formula	$C_{27}H_{16}FeO$	$C_{78}H_{84}Fe_2O_2P_2Pt$	$C_{45}H_{30}AuFeOP$	$C_{28}H_{18}FeHgO$
Molecular weight	412.25	1422.18	870.48	626.86
Crystal size (mm^3)	0.32 × 0.19 × 0.15	0.30 × 0.20 × 0.14	0.22 × 0.13 × 0.07	0.23 × 0.09 × 0.07
Crystal system	Monoclinic	Monoclinic	Triclinic	Monoclinic
Space group	$P2_1/c$	$P\bar{1}$	$P\bar{1}$	$P2_1/c$
a (Å)	11.6923(9)	10.087(2)	9.7888(5)	12.3155(10)
b (Å)	28.279(2)	10.493(2)	12.6542(6)	9.9751(8)
c (Å)	11.6327(10)	16.921(3)	14.9629(7)	17.0672(13)
α (°)		88.46(3)	88.4880(10)	
β (°)	95.763(2)	75.55(3)	74.9320(10)	95.901(2)
γ (°)		81.47(3)	86.0330(10)	
U (Å^3)	3826.9(5)	1715.2(6)	1785.37(15)	2085.6(3)
D_{calc} (g cm^{-3})	1.431	1.377	1.619	1.996
Z	8	1	2	4
μ (Mo–K$_\alpha$) (mm^{-1})	0.803	2.543	4.589	8.066
F(0 0 0)	1696	728	856	1200
θ range (°)	1.75–27.54	1.96–27.50	1.41–25.00	2.37–25.00
Reflections collected	22 617	10 051	8901	10 143
Unique reflections	8584	7335	7488	3648
R_{int}	0.0579	0.0321	0.0131	0.0611
Observed reflections [$I > 2\sigma(I)$]	4153	6486	6620	2213
No. of parameters	523	385	883	281
R_1, wR_2 [$I > 2\sigma(I)$]	0.0441, 0.0787	0.0481, 0.1271	0.0328, 0.0864	0.0429, 0.0854
R_1, wR_2 (all data)	0.1116, 0.0939	0.0530, 0.1306	0.0378, 0.0901	0.0831, 0.0954
Goodness-of-fit on F^2	0.826	1.001	0.920	0.898
Residual extrema in final diff. map (e Å^{-3})	0.393 to −0.363	2.108 to −1.646	1.217 to −0.708	1.337 to −0.841

5. Crystallography

Single crystals of **3**, **5**, **6** and **7** suitable for X-ray crystallographic analyses were chosen and mounted on a glass fiber using epoxy resin. Crystal data and other experimental details are summarized in Table 6. The diffraction experiments were carried out at room temperature on a Bruker Axs SMART 1000 CCD area-detector diffractometer using graphite-monochromated Mo-K$_\alpha$ radiation ($\lambda = 0.71073$ Å). At the end of data collection, no crystal decay was observed. The collected frames were processed with the software SAINT [18a], and an absorption correction was applied (SADABS) [18b] to the collected reflections. The structures were solved by direct methods (for **3**, **6** and **7**) and Patterson method (for **5**), and expanded by difference Fourier syntheses using the software SHELTXL [19]. Structure refinements were made on F^2 by the full-matrix least-squares technique. In each case, all the non-hydrogen atoms were refined with anisotropic displacement parameters. The hydrogen atoms were placed in their ideal positions and not refined.

6. Supplementary material

Crystallographic data (comprising hydrogen atom coordinates, thermal parameters and full tables of bond lengths and angles) for the structural analysis has been deposited with the Cambridge Crystallographic Centre (Deposition No. 193382–193385). Copies of this information may be obtained free of charge from The Director, CCDC, 12 Union Road, Cambridge, CB2 1EZ, UK (Fax: +44-1223-336033; e-mail: deposit@ccdc.cam.ac.uk or www: http://www.ccdc.cam.ac.uk).

Acknowledgements

Financial support from the Faculty Research Grants of Hong Kong Baptist University (FRG/00-01/II-57) is gratefully acknowledged.

References

[1] (a) P. Nguyen, P. Gómez-Elipe, I. Manners, Chem. Rev. 99 (1999) 1515;
(b) R.P. Kingsborough, T.M. Swager, Prog. Inorg. Chem. 48 (1999) 123;
(c) F. Paul, C. Lapinte, Coord. Chem. Rev. 178–180 (1998) 431;
(d) J.-P. Sauvage, J.-P. Collin, J.-C. Chambron, S. Guillerez, C. Coudret, V. Balzani, F. Barigelletti, L. De Cola, L. Flamigni, Chem. Rev. 94 (1994) 993;
(e) V.W.-W. Yam, Chem. Commun. (2001) 789.

[2] (a) R. Ziessel, M. Hissler, A. El-Ghayoury, A. Harriman, Coord. Chem. Rev. 178–180 (1998) 1251;
(b) V. Balzani, A. Juris, M. Venturi, S. Campagna, S. Serroni,

Chem. Rev. 96 (1996) 759;
(c) J.A. McCleverty, M.D. Ward, Acc. Chem. Res. 31 (1998) 842;
(d) M.D. Ward, Chem. Soc. Rev. (1995) 121.

[3] (a) O. Lavastre, J. Plass, P. Bachmann, A. Salaheddine, C. Moinet, P.H. Dixneuf, Organometallics 16 (1997) 184;
(b) Z. Yuan, G. Stringer, I.R. Jobe, D. Kreller, K. Scott, L. Koch, N.J. Taylor, T.B. Marder, J. Organomet. Chem. 452 (1993) 115;
(c) H. Schimanke, R. Gleiter, Organometallics 17 (1998) 275;
(d) K.R. Justin Thomas, J.T. Lin, K.-J. Lin, Organometallics 18 (1999) 5285;
(e) A. Hradsky, B. Bildstein, N. Schuler, H. Schottenberger, P. Jaitner, K.-H. Ongania, K. Wurst, J.-P. Launay, Organometallics 16 (1997) 392;
(f) S.L. Stang, F. Paul, C. Lapinte, Organometallics 19 (2000) 1035;
(g) M. Brady, W. Weng, J.A. Gladysz, J. Chem. Soc. Chem. Commun. (1994) 2655;
(h) K.R. Justin Thomas, J.T. Lin, Y.S. Wen, J. Organomet. Chem. 575 (1999) 301;
(i) N.D. Jones, M.O. Wolf, D.M. Giaquinta, Organometallics 16 (1997) 1352;
(j) M.C.B. Colbert, J. Lewis, N.J. Long, P.R. Raithby, A.J.P. White, D.J. Williams, J. Chem. Soc. Dalton Trans. (1997) 99;
(k) V. Grosshenny, A. Harriman, M. Hissler, R. Ziessel, J. Chem. Soc. Faraday Trans. 92 (1996) 2223;
(l) J.A. Thomas, C.J. Jones, J.A. McCleverty, M.G. Hutchings, Polyhedron 15 (1996) 1409.

[4] (a) K.R. Justin Thomas, J.T. Lin, Y.S. Wen, Organometallics 19 (2000) 1008;
(b) N.D. Jones, M.O. Wolf, Organometallics 16 (1997) 1352;
(c) N.J. Long, A.J. Martin, A.J.P. White, D.J. Williams, M. Fontani, F. Laschi, P. Zanello, J. Chem. Soc. Dalton Trans. (2000) 3387;
(d) N.J. Long, A.J. Martin, R. Vilar, A.J.P. White, D.J. Williams, M. Younus, Organometallics 18 (1999) 4261;
(e) H. Fink, N.J. Long, A.J. Martin, G. Opromolla, A.J.P. White, D.J. Williams, P. Zanello, Organometallics 16 (1997) 2646;
(f) M.C.B. Colbert, D. Hodgson, J. Lewis, N.J. Long, P.R. Raithby, Polyhedron 14 (1995) 2759;
(g) M.C.B. Colbert, A.J. Edwards, J. Lewis, N.J. Long, N.A. Page, D.G. Parker, P.R. Raithby, J. Chem. Soc. Dalton Trans. 17 (1994) 2589;
(h) M.C.B. Colbert, S.L. Ingham, J. Lewis, N.J. Long, P.R. Raithby, J. Chem. Soc. Dalton Trans. 14 (1994) 2215;
(i) S.L. Ingham, M.S. Khan, J. Lewis, N.J. Long, P.R. Raithby, J. Organomet. Chem. 470 (1994) 153.

[5] (a) D. Neher, Macromol. Rapid Commun. 22 (2001) 1365;
(b) N.G. Pschirer, U.H.F. Bunz, Macromolecules 33 (2000) 3961;
(c) B.-J. Jung, J.-I. Lee, H.Y. Chu, L.-M. Do, H.-K. Shim, Macromolecules 35 (2002) 2282;
(d) S. Inaoka, R. Advincula, Macromolecules 35 (2002) 2426;
(e) M.S. Liu, X. Jiang, S. Liu, P. Herguth, A.K.-Y. Jen, Macromolecules 35 (2002) 3532;
(f) B. Tsuie, J.L. Reddinger, G.A. Sotzing, J. Soloducho, A.R. Katritzky, J.R. Reynolds, J. Mater. Chem. 9 (1999) 2189;
(g) K.R. Justin Thomas, J.T. Lin, Y.-Y. Lin, C. Tsai, S.-S. Sun, Organometallics 20 (2001) 2262;
(h) X. Gong, M.R. Robinson, J.C. Ostrowski, D. Moses, G.C. Bazan, A.J. Heeger, Adv. Mater. 14 (2002) 581.

[6] (a) J. Lewis, P.R. Raithby, W.-Y. Wong, J. Organomet. Chem. 556 (1998) 219;
(b) W.-Y. Wong, W.-K. Wong, P.R. Raithby, J. Chem. Soc. Dalton Trans (1998) 2761;
(c) W.-Y. Wong, K.-H. Choi, G.-L. Lu, J.-X. Shi, Macromol. Rapid Commun. 22 (2001) 461;
(d) W.-Y. Wong, G.-L. Lu, K.-H. Choi, J.-X. Shi, Macromolecules 35 (2002) 3506;
(e) W.-Y. Wong, G.-L. Lu, K.F. Ng, C.-K. Wong, K.-H. Choi, J. Organomet. Chem. 637-639 (2001) 159;
(f) W.-Y. Wong, K.-H. Choi, G.-L. Lu, J.-X. Shi, P.-Y. Lai, S.-M. Chan, Z. Lin, Organometallics 20 (2001) 5446.

[7] W.-Y. Wong, G.-L. Lu, K.-F. Ng, K.-H. Choi, Z. Lin, J. Chem. Soc. Dalton Trans. (2001) 3250.

[8] (a) G.E. Coates, C. Parkin, J. Chem. Soc. (1962) 3220;
(b) M.I. Bruce, M.I. Horn, J.G. Matisons, M.R. Snow, Aust. J. Chem. 37 (1984) 1163;
(c) R.J. Cross, M.F. Davidson, A.J. McLennan, J. Organomet. Chem. 265 (1984) C37;
(d) W.J. Hunks, M.-A. MacDonald, M.C. Jennings, R.J. Puddephatt, Organometallics 19 (2000) 5063;
(e) M.I. Bruce, B.C. Hall, B.W. Skelton, M.E. Smith, A.H. White, J. Chem. Soc. Dalton Trans. (2002) 995;
(f) M.J. Irwin, J.J. Vittal, R.J. Puddephatt, Organometallics 16 (1997) 3541;
(g) T.E. Muller, S.W.-K. Choi, D.M.P. Mingos, D. Murphy, D.J. Williams, V.W.-W. Yam, J. Organomet. Chem. 484 (1994) 209;
(h) F. Bolletta, D. Fabbri, M. Lombardo, L. Prodi, C. Trombini, N. Zaccheroni, Organometallics 15 (1996) 2415.

[9] (a) C. Lopez, J. Granell, J. Organomet. Chem. 555 (1998) 211;
(b) J. Burdeniuk, D. Milstein, J. Organomet. Chem. 451 (1993) 213.

[10] (a) D. Osella, L. Milone, C. Nervi, M. Ravera, J. Organomet. Chem. 488 (1995) 1;
(b) D. Osella, R. Gobetto, C. Nervi, M. Ravera, R. D'Amato, M.V. Russo, Inorg. Chem. Commun. 1 (1998) 239.

[11] J.P. Glusker, M. Lewis, M. Rossi, Crystal Structure Analysis for Chemists and Biologists (Chapter 13), VCH Publishers, New York, 1994, p. 548.

[12] (a) E. Gutierrez-Puebla, A. Vegas, S. Garcia-Blanco, Cryst. Struct. Commun. 8 (1979) 861;
(b) E. Gutierrez-Puebla, A. Vegas, S. Garcia-Blanco, Acta Crystallogr. Sect. B 34 (1978) 3382;
(c) B.F. Hoskins, R. Robson, E.E. Sutherland, J. Organomet. Chem. 515 (1996) 259;
(d) C. Hartbaum, G. Roth, H. Fischer, Eur. J. Inorg. Chem. (1998) 191;
(e) I. Ghosh, R. Mishra, D. Poddar, A.K. Mukherjee, Chem. Commun. (1996) 435.

[13] (a) N.W. Alcock, P.A. Lampe, P. Moore, J. Chem. Soc. Dalton Trans. (1980) 1471;
(b) C.A. Ghilardi, S. Midollini, A. Orlandini, A. Vacca, J. Chem. Soc. Dalton Trans. (1993) 3117.

[14] W.L.F. Armarego, D.D. Perrin, Purification of Laboratory Chemicals, fourth ed., Butterworth-Heinemann, Guildford, UK, 1996.

[15] M. Rosenblum, N. Brawn, J. Papenmeier, M. Applebaum, J. Organomet. Chem. 6 (1966) 173.

[16] J. Chatt, B.L. Shaw, J. Chem. Soc. (1960) 4020.

[17] G.B. Kauffman, L.A. Teter, Inorg. Synth. 7 (1963) 245.

[18a] SAINT, Reference manual, Siemens Energy and Automation, Madison, WI, 1994–1996.

[18b] G.M. Sheldrick, SADABS, Empirical Absorption Correction Program, University of Göttingen, 1997.

[19] G.M. Sheldrick, SHELXTL™, Reference manual, ver. 5.1, Madison, WI, 1997.